

Electroweak radiative corrections to neutrino–nucleon scattering at NuTeV

Kwangwoo Park*

Department of Physics, Southern Methodist University, Dallas, TX 75275, USA

Ulrich Baur†

Department of Physics, SUNY at Buffalo, Buffalo, NY 14260, USA

Doreen Wackeroth‡

Department of Physics, SUNY at Buffalo, Buffalo, NY 14260, USA

*Institut für Theoretische Teilchenphysik, Karlsruhe Institute of Technology (KIT),
Universität Karlsruhe, 76128 Karlsruhe, Germany*

A dedicated effort by both the experimental and theoretical communities is crucial for achieving a precise determination of Standard Model parameters such as the W mass (M_W). M_W is measured directly at the CERN LEP2 e^+e^- and the Fermilab Tevatron $p\bar{p}$ colliders, resulting in a precision of $\delta M_W/M_W = 0.03\%$ [1]. A complementary M_W measurement is provided by the NuTeV collaboration [2, 3], who extract $\sin^2 \theta_W$, and thus M_W , from the ratio of deep-inelastic neutral and charged-current neutrino(anti-neutrino)-Nucleon ($\nu N(\bar{\nu}N)$) scattering cross sections. However, their result differs from direct measurements performed at LEP2 and the Tevatron by about three standard deviations [2, 3]. Possible sources for the origin of this discrepancy have been extensively studied in the literature (see, e. g., [4]), among them the impact of electroweak radiative corrections [5, 6, 7]. Here we provide first (preliminary) results of a new calculation of electroweak $\mathcal{O}(\alpha)$ corrections with emphasis on the effects of non-zero muon and charm quark masses. We find non-negligible shifts in $\sin^2 \theta_W$ due to these mass effects but more detailed studies including detector resolution effects are needed to determine their impact on M_W as extracted by the NuTeV collaboration.

I. INTRODUCTION

The Standard Model (SM) represents the best current understanding of electroweak and strong interactions of elementary particles. In recent years it has been impressively confirmed experimentally through the precise determination of W and Z boson properties at the CERN LEP and the Stanford Linear e^+e^- colliders, and the discovery of the top quark at the Fermilab Tevatron $p\bar{p}$ collider.

A precise measurement of M_W does not only provide a further precisely known SM input parameter, but significantly improves the indirect limit on the Higgs-boson mass obtained by comparing SM predictions with electroweak precision data as illustrated in Fig. 1

A measurement of M_W can also be extracted from a measurement of the sine squared of the weak mixing angle, $\sin^2 \theta_W$, via the well-known relation between the W and Z boson masses, $M_W^2 = M_Z^2(1 - \sin^2 \theta_W)$. The NuTeV collaboration extracts M_W from the ratio of neutral and charged-current neutrino and anti-neutrino cross sections [2, 3]. Their results differ from direct measurements performed at LEP2 and the

Tevatron by about 3σ [2, 3] as shown in Fig. 2.

Much effort both experimentally and theoretically has gone into understanding this discrepancy. These efforts include studies of QCD corrections, parton distribution functions, and nuclear structure (see, e. g., [4] for an overview). However, the impact of electroweak radiative corrections has not been fully studied yet. In the extraction of M_W from NuTeV data, only part of the electroweak corrections have been included [8]. Since then the complete calculation of these corrections has been made available in the literature [5, 6, 7], but a realistic, experimental study of their impact on the NuTeV measurement on M_W has not been performed yet.

In order to remedy this situation as a first step we calculated the complete $\mathcal{O}(\alpha)$ contribution to neutrino–nucleon scattering including the full muon and charm-quark mass dependence, which has been neglected in previous studies. Here we present first (preliminary) results of this new calculation with emphasis on these mass effects. A detailed study, also taking into account more realistic detector resolution effects, is work in progress [9].

II. SOME DETAILS OF THE CALCULATION

Our calculation of the complete $\mathcal{O}(\alpha)$ corrections to the neutral-current (NC) and charged-current (CC) $\nu N(\bar{\nu}N)$ scattering processes (the tree-level Feynman

*Electronic address: kpark@smu.edu

†Electronic address: baur@ubhep.physics.buffalo.edu

‡Electronic address: dow@ubpheno.physics.buffalo.edu

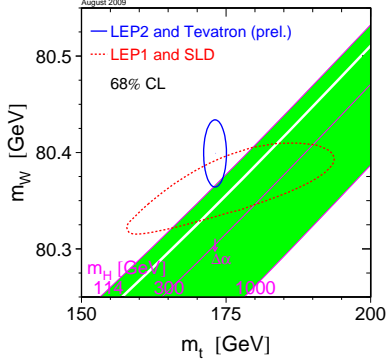


FIG. 1: The SM prediction for M_W with dependence on the top-quark mass (M_t) and Higgs boson mass (M_H), resulting in the shaded band, is compared with the experimental values of M_W and M_t (dotted ellipse) and an indirect measurement from all electroweak precision data (solid ellipse) [1]. Present values of M_W , M_t favor a relatively light SM Higgs, while the NuTeV value of $M_W (= 80.136 \pm 0.084 \text{ GeV})$ [2, 3] prefers a much heavier SM Higgs.

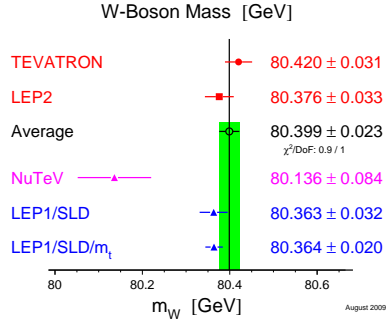


FIG. 2: Direct (Tevatron, LEP2, and NuTeV) and indirect measurements of M_W . The NuTeV value of M_W differs from the world average value by about 3σ [1].

diagrams are shown in Fig. 3) follows closely the treatment of s -channel W and Z production at hadron colliders of [10, 11]. The $\mathcal{O}(\alpha)$ corrections consist of the full set of electroweak one-loop diagrams and real photon radiation from both the external charged fermion legs and the internal W boson in the CC process. As usual, they exhibit UV and IR divergences. UV divergences are canceled by including the counterterms of the on-shell renormalization scheme [12, 13]. By applying the two-cut-off phase-space-slicing method [14], we extract the soft and collinear singularities from the real photonic corrections. We use fermions masses and a fictitious photon mass respectively as regulators for the soft and collinear singularities. The photon mass dependence cancels in the sum of virtual and real soft-photon radiation, but mass singularities of the form

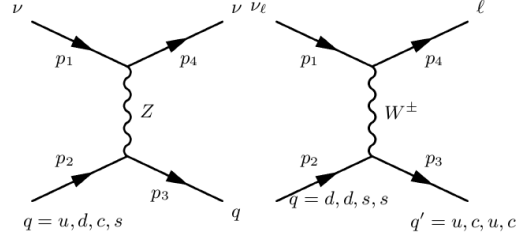


FIG. 3: Feynman diagrams for the tree-level NC (left) and CC (right) νN scattering processes.

$\log(\hat{t}/m_f^2)$ may survive, which arise when the photon is emitted collinear with the charged fermion. In the case of final-state photon radiation, in inclusive observables these mass singularities cancel against the loop-Born interference. However, mass singularities connected to initial-state photon radiation survive in general. These need to be absorbed in the parton distribution functions (PDF), which can be done in analogy to gluon radiation in QCD. Finally, the numerical phase space integration was done using Monte Carlo techniques based on the Vegas algorithm [15].

After convolution with the quark PDFs, the predictions for the hadronic, electroweak (EW) next-to-leading order (NLO) cross section for νN scattering is obtained as follows:

$$\begin{aligned} d\sigma_{NC,CC}^{\nu}(E_{\nu}) = & \sum_i \int dx q_i(x, Q^2) (d\hat{\sigma}_{0,(NC,CC)}^{\nu} + d\hat{\sigma}_{v+s}^{NC,CC}) \\ & + \sum_i \int_x^{1-\delta_s} \frac{dz}{z} q_i\left(\frac{x}{z}, Q^2\right) d\hat{\sigma}_c^{NC,CC} \\ & + \sum_i \int dx q_i(x, Q^2) d\hat{\sigma}_h^{NC,CC}, \end{aligned} \quad (1)$$

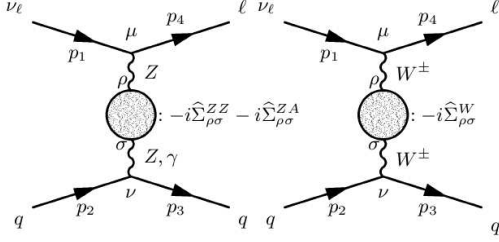
where the parton level cross section consists of tree-level, virtual, soft and collinear $\mathcal{O}(\alpha)$ contributions (including the PDF counterterms) and the real hard photon radiation contribution.

A. Fermion-mass effects

We performed the calculation with and without including fermion-mass effects and are considering the following two cases:

- case 1: All external fermions are considered to be massless and we only keep non-zero fermion masses as regulators of the collinear singularities.
- case 2: The full muon and charm-quark mass dependence is taken into account, but light external fermions are treated as in the first case.

Fermion-mass effects in EW radiative corrections may not be numerically negligible in this process, since


 FIG. 4: Feynman diagrams for self-energy corrections to the NC and CC νN production processes.

the relevant parton-level energy scale ($q^2 = \hat{t}$) can be of the same order of magnitude. This is illustrated below on the example of the W self-energy correction ($\hat{\Sigma}_{\rho\sigma}^W$) to the CC process shown in Fig. 4. Its contribution to the one-loop corrected matrix element at $\mathcal{O}(\alpha)$ reads

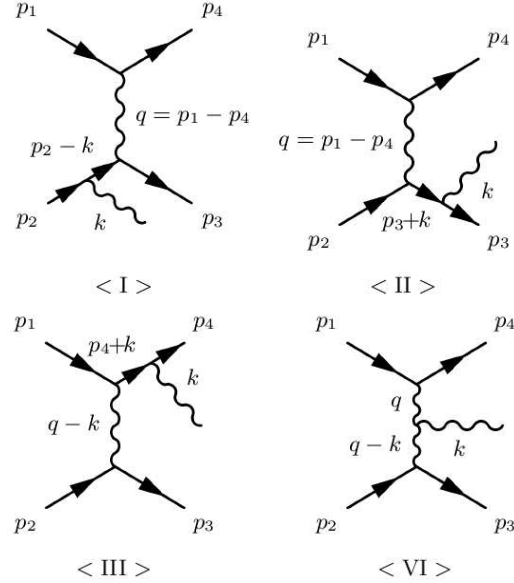
$$\mathcal{M}_{virt}^{CC} = \frac{-e^2}{8s_W^2} \frac{g^{\mu\rho} \hat{\Sigma}_{\rho\sigma}^W g^{\sigma\nu}}{(q^2 - M_W^2)^2} [\bar{u}_4 \gamma_\mu (1 - \gamma_5) u_1] [\bar{u}_3 \gamma_\nu (1 - \gamma_5) u_2]. \quad (2)$$

With the renormalized self energy $\hat{\Sigma}_{\rho\sigma}^W$ being decomposed in transverse and longitudinal parts, $\hat{\Sigma}_{\rho\sigma}^W = \left(g_{\rho\sigma} - \frac{q_\rho q_\sigma}{q^2}\right) \hat{\Sigma}_T^W + \frac{q_\rho q_\sigma}{q^2} \hat{\Sigma}_L^W$, one finds the following contribution to the NLO matrix element squared:

$$2\text{Re}\mathcal{M}_{LO}^{CC*} \mathcal{M}_{virt}^{CC} = - \underbrace{\frac{2e^4(p_1 \cdot p_2 p_3 \cdot p_4)}{s_W^4 (\hat{t} - M_W^2)^2}}_{=|\mathcal{M}_0|^2} \left[\frac{2\text{Re}\hat{\Sigma}_T^W}{(\hat{t} - M_W^2)} + \frac{m_4^2 (m_2^2 p_1 \cdot p_3 - m_3^2 p_1 \cdot p_2) \text{Re}(\hat{\Sigma}_L^W - \hat{\Sigma}_T^W)}{2\hat{t} (\hat{t} - M_W^2)} \right]. \quad (3)$$

If we consider massless fermions for the external legs (case 1), the second term in Eq. (3) vanishes. However, for massive fermions (case 2) the longitudinal two-point function contributes to the physical cross section. Since we work in the Feynman-'t Hooft gauge, we also had to include the contributions from the would-be Goldstone bosons, which are not explicitly shown here. In the s -channel W production process such as gauge-boson production in Drell-Yan processes at the Tevatron and the LHC, \hat{t} is replaced with \hat{s} , so that the second term is usually negligible. In t -channel deep inelastic scattering, however, these fermion-mass effects deserve a closer investigation, especially in the small \hat{t} region, corresponding to a small momentum fraction x . Note that similar effects also arise from vertex and box corrections.

In case of real photon radiation amplitude-level fermion-mass effects only arise in the CC νN scatter-


 FIG. 5: Feynman diagrams for real photon radiation in the CC νN scattering process.

ing process (the matrix elements to real photon radiation in the NC process of cases 1 and 2 are identical), and only due to the ϕ^\pm exchange diagrams which are suppressed by $\mathcal{O}(m_f^2/M_W^2)$. The Feynman diagrams are shown in Fig. 5 and the corresponding matrix element (\mathcal{M}_r) can be written in terms of for $U(1)$ -conserved leptonic and hadronic currents as follows ($\epsilon_\rho(k)$ denotes the photon polarization vector):

$$\mathcal{M}_r = \frac{e^3}{8s_w^2} \left[\frac{\mathcal{M}_{had}^{CC,\rho}}{(\hat{t} - M_W^2)} + \frac{\mathcal{M}_{lept}^{CC,\rho}}{(\hat{t} - M_W^2 - 2k \cdot q)} \right] \epsilon_\rho^*(k) \quad (4)$$

with
hadronic current

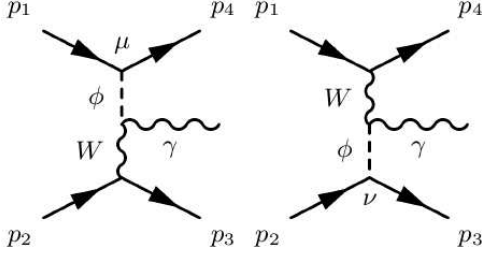
$$\mathcal{M}_{had}^{CC,\rho} = [\bar{u}_4 \gamma_\mu (1 - \gamma_5) u_1] [\bar{u}_3 (\Gamma_I^{\mu\rho} + \Gamma_{II}^{\mu\rho} + \Gamma_{N_1}^{\mu\rho}) (1 - \gamma_5) u_2] + \mathcal{J}_m^{\rho'}$$

leptonic current

$$\mathcal{M}_{lept}^{CC,\rho} = [\bar{u}_4 (\Gamma_{III}^{\mu\rho} + \Gamma_{N_2}^{\mu\rho}) (1 - \gamma_5) u_1] [\bar{u}_3 \gamma^\mu (1 - \gamma_5) u_2] - \mathcal{J}_m^{\rho'}$$

with,

$$\begin{aligned} \Gamma_I^{\mu\rho} &= Q_2 \gamma^\mu \frac{p_2^\rho - \not{k} \gamma^\rho / 2}{-k \cdot p_2}, & \Gamma_{II}^{\mu\rho} &= Q_3 \frac{p_3^\rho + \gamma^\rho \not{k} / 2}{k \cdot p_3} \gamma^\mu \\ \Gamma_{III}^{\mu\rho} &= Q_4 \frac{p_4^\rho + \gamma^\rho \not{k} / 2}{k \cdot p_4} \gamma^\mu, & \Gamma_{N_1}^{\mu\rho} &= \frac{\gamma^\mu q^\rho + \gamma^\rho k^\mu - g^{\mu\rho} \not{k}}{-k \cdot q} \\ \Gamma_{N_2}^{\mu\rho} &= \frac{\gamma^\mu q^\rho - \gamma^\rho k^\mu g^{\mu\rho} \not{k}}{k \cdot q}, & q^\mu &= p_1^\mu - p_4^\mu \end{aligned}$$

Feynman Rules at μ and ν

$$\mu : \frac{-ie}{2\sqrt{2}s_w M_W} (m_4(1 - \gamma_5) - m_1(1 + \gamma_5))$$

$$\nu : \frac{ie}{2\sqrt{2}s_w M_W} (m_3(1 - \gamma_5) - m_2(1 + \gamma_5))$$

FIG. 6: Feynman diagrams for the contribution of ϕ scalar boson to real photon radiation in the CC νN scattering process, and their Feynman rules

$$\mathcal{J}_m^\rho = \frac{1}{2k \cdot q} \left(m_1 [\bar{u}_4(1 + \gamma_5)u_1] [\bar{u}_3 \gamma^\rho (1 - \gamma_5)u_2] \right. \\ \left. - m_4 [\bar{u}_4(1 - \gamma_5)u_1] [\bar{u}_3 \gamma^\rho (1 - \gamma_5)u_2] \right. \\ \left. - m_2 [\bar{u}_4 \gamma^\rho (1 - \gamma_5)u_1] [\bar{u}_3(1 + \gamma_5)u_2] \right. \\ \left. + m_3 [\bar{u}_4 \gamma^\rho (1 - \gamma_5)u_1] [\bar{u}_3(1 - \gamma_5)u_2] \right).$$

where the subscripts, I, II, III, and IV correspond to the diagrams shown in Fig. 5. In both massless and massive case, \mathcal{J}_m^ρ vanishes when we include the contribution of ϕ scalar boson for the massive case as illustrated in Fig. 6.

B. Treatment of numerical instabilities

It is well-known (see, e. g., [5]) that the EW NLO cross section to the NC process suffers from a numerical instability at small values of \hat{t} owing to the photon exchange diagram shown in Fig. 3. As a remedy of this kind of instability, we apply a Taylor expansion around small \hat{t} . In Fig. 7 we illustrate the stability of this expansion.

Box corrections exhibit numerical instabilities originating from vanishing Gram determinants at small kinematic variables when the standard Passarino-Veltman reduction formalism [16] is employed to determine the coefficient functions of vector and tensor four-point integrals. Especially, the crossed box contribution in the low x -region suffers from these instabilities which can be traced back to numerical unstable coefficients of three-point integrals. In the following we present a reduction formalism which yields stable results as illustrated in Fig. 8 for case 1 (see also [19] for an alternate solution). In phase-space regions of

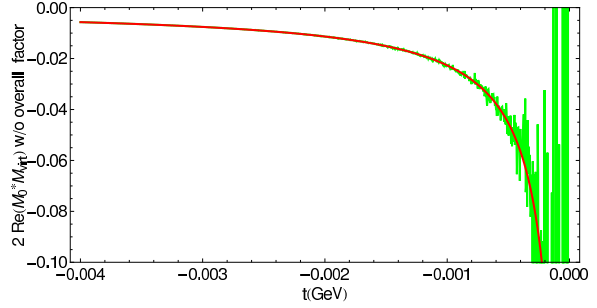


FIG. 7: Numerical instability appears in fermion-fermion-photon exchange vertex loop (green curve) owing to photon propagator, while Taylor expansion shows numerical stability (red curve).

small kinematic variables, the coefficients of the three-point vector and tensor integral

$$C^\mu, C^{\mu\nu} = \frac{(2\pi\mu)^{4-D}}{i\pi^2} \int d^D q \frac{q^\mu, q^\mu q^\nu}{[q^2 - m_0^2][(q+p_1)^2 - m_1^2][(q+p_2)^2 - m_2^2]},$$

defined as

$$C^\mu = p_1^\mu C_1 + p_2^\mu C_2, \\ C^{\mu\nu} = g^{\mu\nu} C_{00} + p_1^\mu p_2^\nu C_{12} + p_2^\mu p_1^\nu C_{21} + p_1^\mu p_1^\nu C_{11} + p_2^\mu p_2^\nu C_{22},$$

can be approximated in terms of two-point functions as follows

$$C_1 = \alpha B_1^1 + 2\alpha^2 [B_{00}^1 - B_{00}^2 + (p_1^2 - p_1 \cdot p_2) B_{11}^1] \\ + \mathcal{O}((p_1^2)^2, (p_2^2)^2, (p_1 \cdot p_2)^2) \\ C_2 = -\alpha B_1^2 + 2\alpha^2 [B_{00}^2 - B_{00}^1 + (p_2^2 - p_1 \cdot p_2) B_{11}^2] \\ + \mathcal{O}((p_1^2)^2, (p_2^2)^2, (p_1 \cdot p_2)^2)$$

$$C_{00} = \alpha(B_{00}^1 - B_{00}^2) + 2\alpha^2 [(p_1^2 - p_1 \cdot p_2) B_{00}^1 \\ + (p_2^2 - p_1 \cdot p_2) B_{00}^2] + \mathcal{O}((p_1^2)^2, (p_2^2)^2, (p_1 \cdot p_2)^2)$$

$$C_{11} = \alpha(B_{11}^1) + 2\alpha^2 [2B_{00}^1 + (p_1^2 - p_1 \cdot p_2) B_{11}^1] \\ + \mathcal{O}((p_1^2)^2, (p_2^2)^2, (p_1 \cdot p_2)^2)$$

$$C_{12} = C_{21} = -2\alpha^2 [B_{00}^1 + B_{00}^2] \\ + \mathcal{O}((p_1^2)^2, (p_2^2)^2, (p_1 \cdot p_2)^2)$$

$$C_{22} = -\alpha(B_{11}^2) + 2\alpha^2 [2B_{00}^2 + (p_2^2 - p_1 \cdot p_2) B_{11}^2] \\ + \mathcal{O}((p_1^2)^2, (p_2^2)^2, (p_1 \cdot p_2)^2)$$

and the scalar three-point integral reads:

$$C_0 = \alpha(B_0^1 - B_0^2) + 2\alpha^2 [(p_1^2 - p_1 \cdot p_2) B_1^1 + (p_2^2 - p_1 \cdot p_2) B_1^2] \\ + \mathcal{O}((p_1^2)^2, (p_2^2)^2, (p_1 \cdot p_2)^2) \quad (5)$$

with α and B -functions that are defined as,

$$\alpha = \frac{1}{m_1^2 - m_2^2 - p_1^2 + p_2^2}, \quad B_{\mu\nu\dots}^i = B_{\mu\nu\dots}(p_i^2, m_0^2, m_i^2).$$

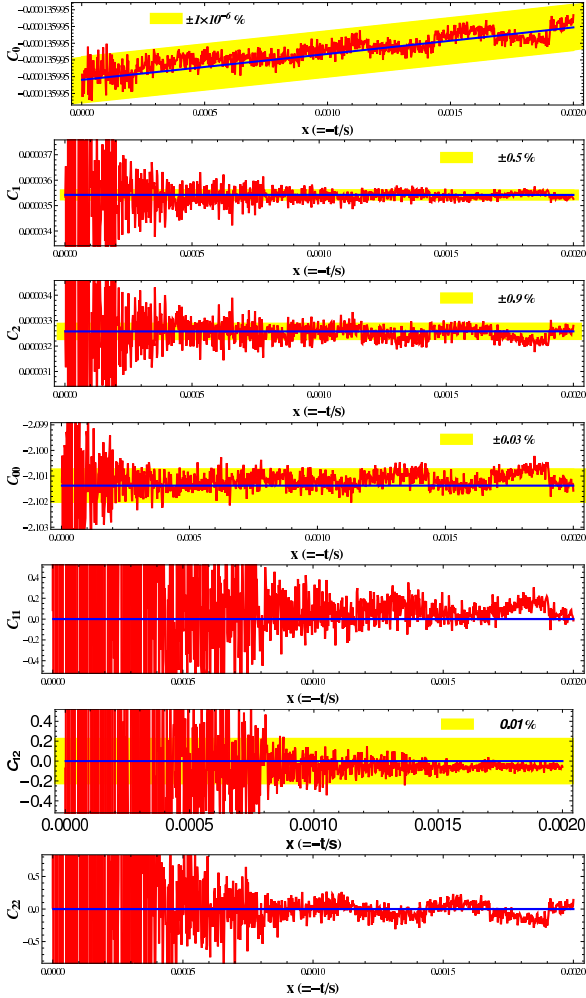


FIG. 8: The standard Passarino-Veltman reduction exhibits a numerical instability (red curve) while Eq. (5) provides stable results (blue curve).

The detailed derivation of these expressions can be found in [17]. In Fig. 8 we show a comparison of these two derivations of the C_{ij} functions in the critical phase space region, i. e. at small x .

III. NUMERICAL RESULT

The measured value of $\sin^2 \theta_W$ can be extracted from Paschos' ratio [18]

$$R = \frac{\sigma_{NC}^\nu(\nu N \rightarrow \nu X) - \sigma_{NC}^\nu(\bar{\nu} N \rightarrow \bar{\nu} X)}{\sigma_{CC}^\nu(\nu N \rightarrow \ell X) - \sigma_{CC}^\nu(\bar{\nu} N \rightarrow \bar{\ell} X)} = \rho^2 \left(\frac{1}{2} - \sin^2 \theta_W \right) \quad (6)$$

In the on-mass-shell renormalization scheme, $\sin^2 \theta_W$ is related to the masses of both W and Z bosons as

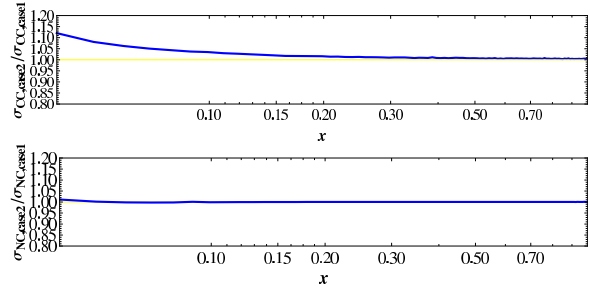


FIG. 9: Ratio of νN scattering cross sections calculated with massless and massive external fermions for both CC and NC production processes.

follows:

$$\sin^2 \theta_W = 1 - \frac{M_W^2}{M_Z^2}. \quad (7)$$

In order to determine the impact of the higher-order corrections under investigation on the extracted value of $\sin^2 \theta_W$, we use the following expression suggested by [8]:

$$\Delta \sin^2 \theta_W = \frac{\frac{1}{2} - \sin^2 \theta_W + \frac{20}{27} \sin^4 \theta_W}{1 - \frac{40}{27} \sin^2 \theta_W} (\delta R_{NC}^\nu + \delta R_{CC}^\nu), \quad (8)$$

where the ratios of δR_{NC}^ν , δR_{CC}^ν and R_0^ν are defined as

$$R_0^\nu = \frac{\sigma_{0,NC}^\nu}{\sigma_{0,CC}^\nu}, \quad \delta R_{NC}^\nu = \frac{\delta \sigma_{NC}^\nu}{\sigma_{NC}^\nu}, \quad \delta R_{CC}^\nu = -\frac{\delta \sigma_{CC}^\nu}{\sigma_{CC}^\nu}.$$

For the numerical evaluation we use the same in [5].

As discussed earlier, for the massless calculation (case 1), we neglect fermion masses whenever it is possible, i. e. we take their masses only for regularizing singularities, while, in the massive case (case 2), we keep the muon and charm-quark masses. Note that following results are *preliminary*. As can be seen in Fig. 9, where we compare the νN scattering cross sections calculated in both cases for both CC and NC production processes, fermion-mass effects are only visible at small x and are more pronounced in the CC case. How this may translate into the extracted value of $\sin^2 \theta_W$ is illustrated in Tab. I. More detailed studies are under way.

TABLE I: Preliminary results obtained with the *MRST2004QED* PDF set and a cut on $y = -\hat{t}/\hat{s} \geq 0.12$.

	R_0^ν	δR_{NC}^ν	δR_{CC}^ν	$\Delta \sin^2 \theta_W$
Case 1	0.30638	0.0527	-0.0916	-0.0182
Case 2	0.31477	0.0548	-0.1059	-0.0258

IV. CONCLUSION

Deep-inelastic neutrino–nucleon scattering provides an excellent testing ground for the electroweak SM, complementary to e^+e^- and hadronic colliders. Measurements of electroweak parameters in neutrino–nucleon scattering are not only comparable in precision but they also probe the EW SM at many orders of magnitude in $\hat{t} = q^2$, i.e. the parton-level momentum transfer in these processes.

The NuTeV collaboration used the calculation of [8], which is based on a massless fermion approximation, and did not include the entire set of electroweak $\mathcal{O}(\alpha)$ corrections. Seventeen years later, a complete calculation of the $\mathcal{O}(\alpha)$ corrections to neutrino–nucleon scattering became available [5]. In a follow-up paper [7], leading higher order corrections, i.e. beyond one-loop, have been included as well. In [5], the discussion focused on the EW input scheme dependence of $\sin^2 \theta_W$ measured in neutrino–nucleon scattering. They concluded that the theoretical uncertainty due to missing higher-order corrections has been underestimated by the NuTeV collaboration, and, thus, is a potential source for at least part of the observed discrepancy.

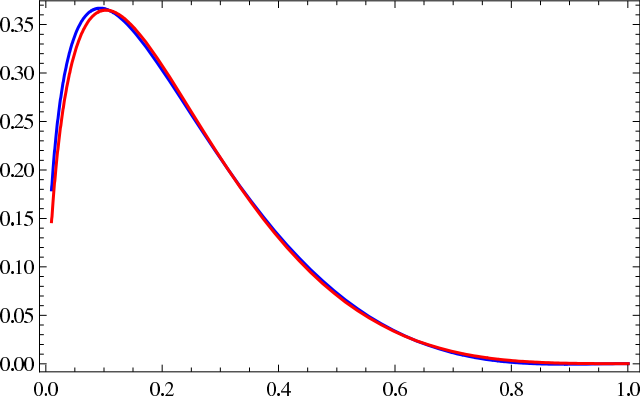
In this study we focus on another potential source of a theoretical uncertainty, which has not been considered before. i.e. the effects of muon and charm-quark masses in the calculation of electroweak corrections.

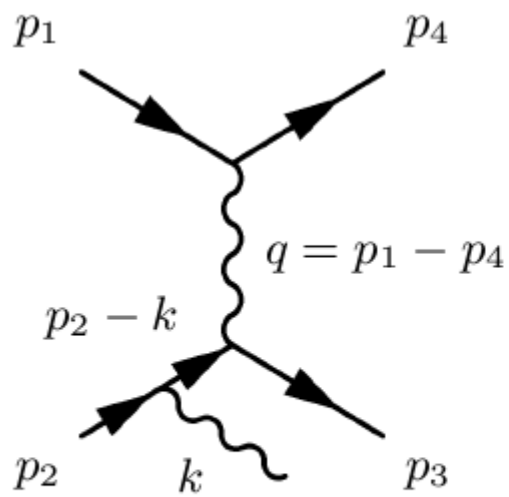
We calculated the complete electroweak $\mathcal{O}(\alpha)$ corrections to neutrino–nucleon scattering with and without taking into account these fermion-mass effects. We studied their impact on $\sin^2 \theta_W$ as extracted from the νN scattering cross section by the NuTeV collaboration. We found non-negligible differences in $\sin^2 \theta_W$ when using our calculation with and without considering non-zero muon and charm-quark masses. However, a more realistic study is needed including a simulation of the detector resolution, for instance, to determine whether these effects can account for part of the NuTeV anomaly. Such a study is work in progress and will be performed in collaboration with the NuTeV collaboration.

Acknowledgments

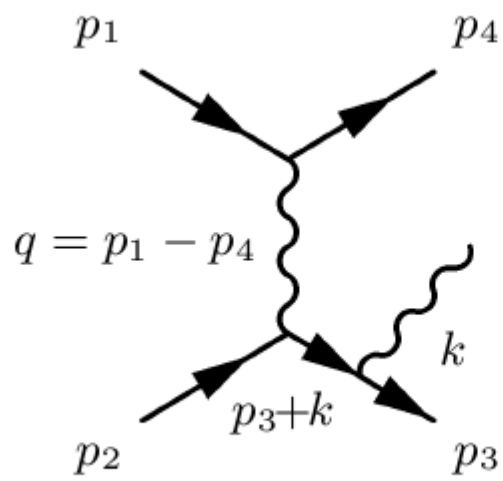
We are grateful to Kevin McFarland for fruitful discussions and guidance concerning experimental issues. The work of K. P. is supported by the U.S. Department of Energy under grant DE-FG02-04ER41299. This research is also supported by the National Science Foundation under grants No. NSF-PHY-0547564 and NSF-PHY-0757691. The work of D. W. is presently also supported by a DFG Mercator Visiting Professorship.

-
- [1] ALEPH Collaboration and CDF Collaboration and D0 Collaboration and DELPHI Collaboration and L3 Collaboration and OPAL Collaboration and SLD Collaboration and LEP Electroweak Working Group and Tevatron Electroweak Working Group and SLD Electroweak Working Group and Heavy Flavour Group, arXiv:0811.4682 [hep-ex], update taken from <http://lepewwg.web.cern.ch/LEPEWWG/plots/summer2009>.
 - [2] G. P. Zeller *et al.* [NuTeV Collaboration], Phys. Rev. Lett. **88**, 091802 (2002) [Erratum-ibid. **90**, 239902 (2003)] [arXiv:hep-ex/0110059].
 - [3] G. P. Zeller [NuTeV Collaboration], arXiv:hep-ex/0207037.
 - [4] K. S. McFarland and S. O. Moch, arXiv:hep-ph/0306052.
 - [5] K. P. O. Diener, S. Dittmaier and W. Hollik, Phys. Rev. D **69**, 073005 (2004) [arXiv:hep-ph/0310364].
 - [6] A. B. Arbuzov, D. Y. Bardin and L. V. Kalinovskaya, JHEP **0506**, 078 (2005) [arXiv:hep-ph/0407203].
 - [7] K. P. Diener, S. Dittmaier and W. Hollik, Phys. Rev. D **72**, 093002 (2005) [arXiv:hep-ph/0509084].
 - [8] D. Y. Bardin and V. A. Dokuchaeva, JINR-E2-86-260.
 - [9] U. Baur, K. McFarland, K. Park, and D. Wackeroth, in preparation.
 - [10] U. Baur, S. Keller and D. Wackeroth, Phys. Rev. D **59**, 013002 (1999) [arXiv:hep-ph/9807417].
 - [11] U. Baur, O. Brein, W. Hollik, C. Schappacher and D. Wackeroth, Phys. Rev. D **65**, 033007 (2002) [arXiv:hep-ph/0108274].
 - [12] M. Bohm, H. Spiesberger and W. Hollik, Fortsch. Phys. **34**, 687 (1986).
 - [13] A. Denner, Fortsch. Phys. **41**, 307 (1993) [arXiv:0709.1075 [hep-ph]].
 - [14] B. W. Harris and J. F. Owens, Phys. Rev. D **65**, 094032 (2002) [arXiv:hep-ph/0102128].
 - [15] G. P. Lepage, J. Comput. Phys. **27**, 192 (1978).
 - [16] G. Passarino and M. J. G. Veltman, Nucl. Phys. B **160**, 151 (1979).
 - [17] K. Park, “Reduction of one loop integrals,” (in preparation).
 - [18] E. A. Paschos and L. Wolfenstein, Phys. Rev. D **7**, 91 (1973).
 - [19] A. Denner and S. Dittmaier, Nucl. Phys. B **734**, 62 (2006) [arXiv:hep-ph/0509141].

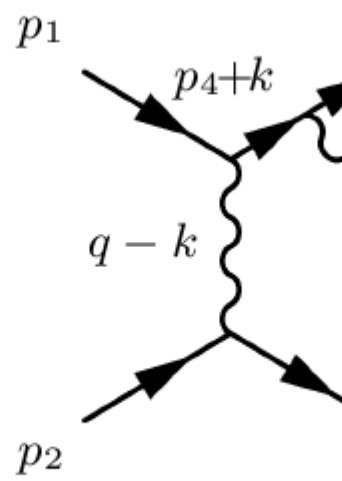




< I >



< II >



< III >